Electronic Supporting Information

Macrocyclic cyanocobalamin (vitamin B_{12}) as a homogeneous electrocatalyst for water oxidation under neutral conditions

Hossain M. Shahadat,†[abc] Hussein A. Younus,†[ef] Nazir Ahmad,[g] Zhang Shiguo,*[e] Serge Zhuiykov,[d] and Francis Verpoort*[abd]

[a] *State Key Laboratory of Advanced Technology for Materials Synthesis and Processing, Wuhan University of Technology, Wuhan 430070, China*

[b] *School of Material Science and Engineering, Wuhan University of Technology, Wuhan 430070, China*

[c] *Department of Chemistry, Faculty of Science, Comilla University, Comilla 3506, Bangladesh*

[d] *Ghent University, Global Campus Songdo, 119 Songdomunhwa-Ro, Yeonsu-Gu, Incheon, Korea*

[e] *College of Materials Science and Engineering, Hunan province key laboratory for advanced carbon materials and applied technology, Hunan University, Changsha 410082, China*

[f] *Chemistry Department, Faculty of Science, Fayoum University, Fayoum 63514, Egypt*

[g] *Department of Chemistry, GC University Lahore, Lahore 54000, Pakistan*

***Author for correspondence.** francis.verpoort@ugent.be

†These authors contributed equally to this work.

‡Electronic supplementary information (ESI) available: CV, FE (%), UV–Vis, ESI–MS, SEM, and EDX figures. For ESI see DOI: 10.1039/x0xx00000x

UV–Vis absorption spectra. The cells for UV–Vis spectrometer (Shimadzu UV–1800) were cleaned by ethanol, acetone, and ultrapure water, respectively.

High resolution of ESI-MS. High resolution of ESI-MS were recorded on a Thermo Scientific Exactive Plus spectrometer at room temperature.

3 Electrodes. Prior to experiments, the GC electrode (0.07 cm^2) was polished with 0.3, 0.1 and 0.05 μm Al_2O_3 slurry for 60 s each to obtain a mirror surface, followed by sonication in ethanol, acetone and distilled water for ~ 60 seconds each to remove debris, and was thoroughly rinsed with ultrapure water (Millipore MilliQ® A10 gradient, 18.25 MΩ cm, 2–4 ppb total organic content). The platinum wire counter electrode was flame annealed and washed with pure water before placing it into the cell. The reference electrode Ag/AgCl (3.0 M KCl) was washed by ultrapure water before every measurement.

FTO Electrode (0.8 cm^2). The FTO glass slide electrode (*R*s ~7 Ω/sq; 0.8 cm^2) was purchased from Zhuhai Kaivo Electronic Components Co., Ltd were cleaned by sonication in detergents, ethanol, and acetone, and ultimately washed with ultra-pure water (Millipore MilliQ® A10 gradient, 18.25 MΩ cm, 2–4 ppb total organic content).

Cyclic voltammetry (CV). Electrochemical workstation (CHI660E) from CH Instruments, Shanghai, China was used in all electrochemical measurements. CV measurements were conducted with three electrode system under an air atmosphere without deaeration. All experiments were performed at room temperature (25 ^oC).

Controlled potential electrolysis (CPE). Long-term CPE (11 h) made in water was performed in a three-compartment electrochemical cell except for the measurement of Faradaic efficiency (%). A FTO was used as the working electrode for electrolysis conducted in aqueous media. The auxiliary electrode was a Pt wire and the reference electrode was a Ag/AgCl electrode. The sample was bubbled with Ar for 30 min before measurement and the CPE experiment was carried out under Ar (purity ~99.999%) with constantly stirring.

Determination of Faradaic Efficiency. An air-tight electrochemical cell containing 1.0 mM vitamin B_{12} in 0.1 M NaPi buffer (pH = 7.0, 20 mL) was sealed with a parafilm and deaerated for 30 min with Ar. Bulk electrolysis was performed at an applied potential of 1.50 V *vs*. Ag/AgCl for 1 h with a FTO electrode under Ar atmosphere. The O_2 content in the headspace of the cell was determined by gas chromatogram with thermal-conductivity detector (GC-TCD) using the steady-state current obtained from CPE (Fig. 3) and the background O_2 from cell leakage was deducted from the total content of O_2. Faradaic efficiency was determined (Fig. S8; 97.5%) by comparing the detected oxygen (DO) amount by

GC-TCD with the theoretical oxygen (TO) amount calculated from the total consumed charge during electrolysis (FE = DO/TO × 100%).

Experimental Section

Materials and methods

Vitamin B_{12} (98%) was purchased from commercial suppliers (Aladdin Chemical Company Ltd.) and used as received without further purification. Aqueous NaPi buffer solutions at different pH were prepared in the laboratory by using chemicals from commercial suppliers with ultra−pure water (Millipore MilliQ® A10 gradient, 18.25 MΩ cm, 2–4 ppb total organic content) and adjusted electrolyte pH with 1.0 M solution of H_3PO_4/NaOH. ^{1}H NMR spectrum of the complex was recorded at different time intervals on a Bruker 500 MHz NMR spectrometer using D_2O solvent and TMS as an internal standard. ESI–MS measurements were recorded on a Bruker Daltonics microTOF–QII spectrometer with electrospray ionization and time–of–flight system, while the Bruker Autoflex 3 was used for MALDI–TOF–MS. FT–IR spectra were recorded on a Bruker Vertex 80 V FT–IR spectrometer. UV−Vis absorption spectra were recorded on a Shimadzu UV−1800 spectrometer at room temperature. SEM images and EDX spectra were taken by TESCAN MIRA3 microscope and Oxford X-Max 50 spectrometer, respectively. All the electrochemical measurements were performed on a CHI660E electrochemical workstation at room temperature with a three–electrode system, including a glassy carbon (GC; 0.07 cm^2)/FTO (*R*s ∼7 Ω/sq; 0.8 cm^2) as the working electrode, a Pt wire as the counter electrode, and a Ag/AgCl (3.0 M KCl) as the reference electrode. All the potentials are referred to the Ag/AgCl electrode, the stability of which was checked periodically during the experiment.

Table S1. A comparison of the catalytic activity of vitamin B_{12} with those of reported homogeneous Co-catalysts

homogeneous Co-based catalyst	conc. & types of buffer	pH	overpotential (V)	j (mA/cm^2) at 1.70 *vs*. NHE	ref.
vitamin B_{12} (experimental)	**0.1 M NaPi**	**7.0**	**0.58**	**1.38**	---
$[(TPA)Co(\mu\text{-}OH)(\mu\text{-}O_2)Co(TPA)](ClO_4)_3$ (TPA = tris(2-pyridylmethyl)amine)	0.1 M Borate	8.0	0.54	1.11	1
$[Co_2(\mu\text{-}OH)_2(TPA)_2](ClO_4)_4$	0.05 M Borate	7.9	0.434	0.50	2
$L^{CH}2^{PO(OH)}2$–Co (L = 5,15-bis-(pentafluorophenyl)-10-(4-dibenzofuran)corrole)	0.1 M NaPi	7.0	0.45	0.49	3
$[Co^{III}\text{-}bTAML]^-$ (bTAML = biuret-modified tetraamidomacrocyclic)	0.1 M NaPi	9.2	1.0	1.49	4
$[Co^{III}_4(\mu\text{-}O)_4(\mu\text{-}OAc)_4(p\text{-}NC_5H_4X)_4]$ (X = H, Me, *t*-Bu, OMe, Br, COOMe, CN)	0.2 M NaPi	7.0	0.50~0.57	0.85	5
$[Co_4(H_2O)_2(PW_9O_{34})_2]^{10-}$ (comprising Co_4O_4)	0.03 M NaPi	8.0	0.54	2.47	6
$[Co_4(H_2O)_4(HPMIDA)_2(PMIDA)_2]^{6-}$ (PMIDA = *N*-(Phosphonomethyl)iminodiacetic acid	0.08 M Borate	**9.0**	0.40	4.33	7
Co-porphyrin	**0.2 M** NaPi	7.0	0.30	7.41	8

Figures Obtained from Experimental Results:

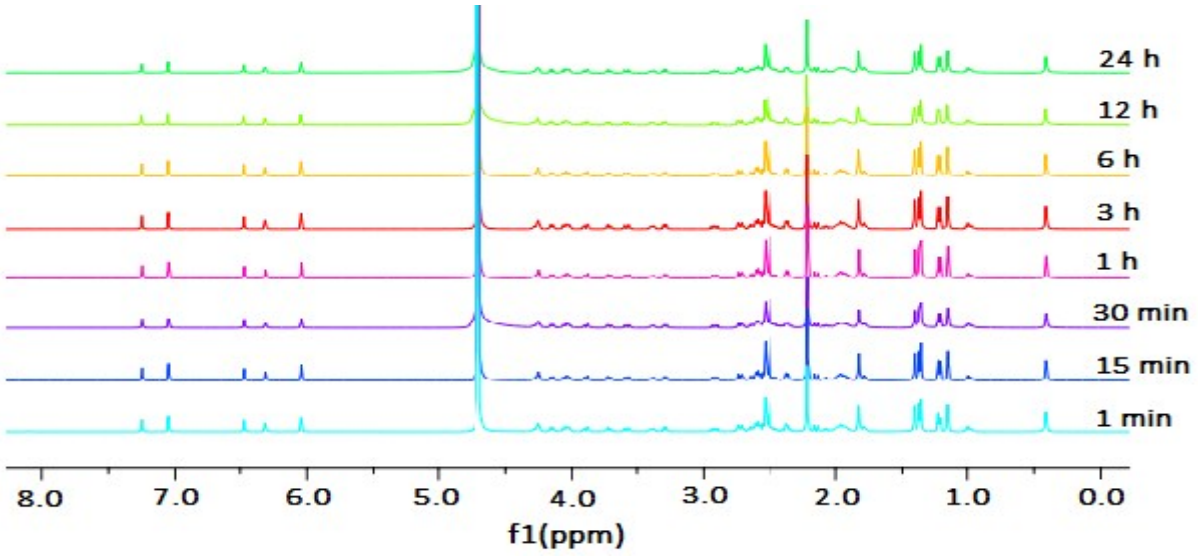

Figure S1. ^{1}H NMR spectra of vitamin B_{12} in D_2O at different time intervals at least up to 24 h.

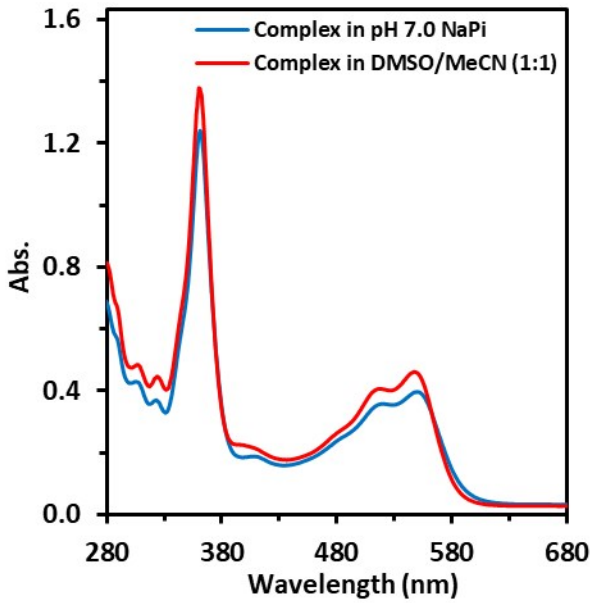

Figure S2. UV–Vis absorption spectra of vitamin B_{12} in organic solvent mixture of DMSO/MeCN (1:1) and 0.1 M aqueous NaPi buffer at pH 7.0.

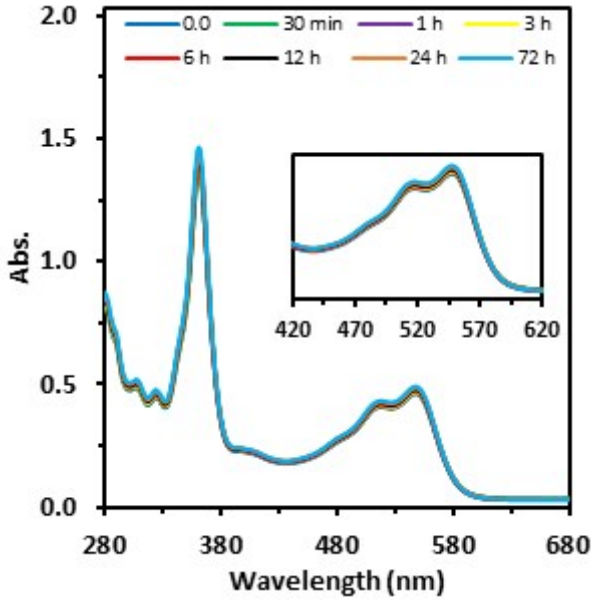

Figure S3. Time–dependent UV–Vis absorption spectra of vitamin B_{12} over 72 h in organic solvent mixture of DMSO/MeCN (1:1).

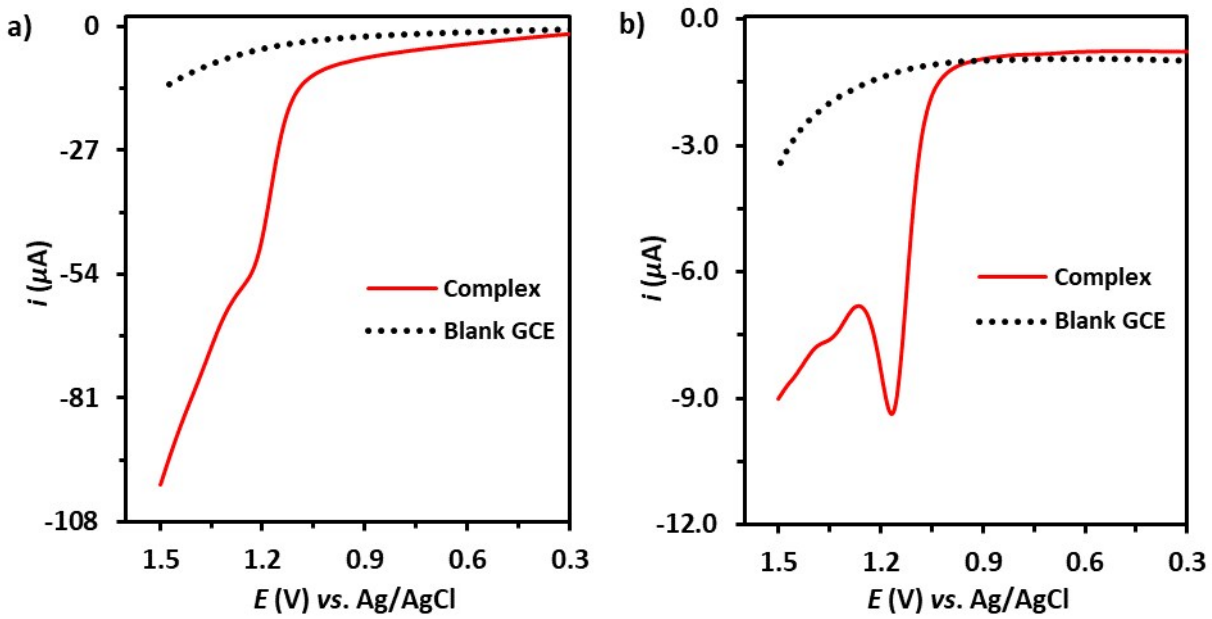

Figure S4. LSVs (a) and DPVs (b) of 1.0 mM vitamin B_{12} complex in 0.1 M aqueous NaPi buffers at pH 7.0 with a GC (0.07 cm^2) as working electrode.

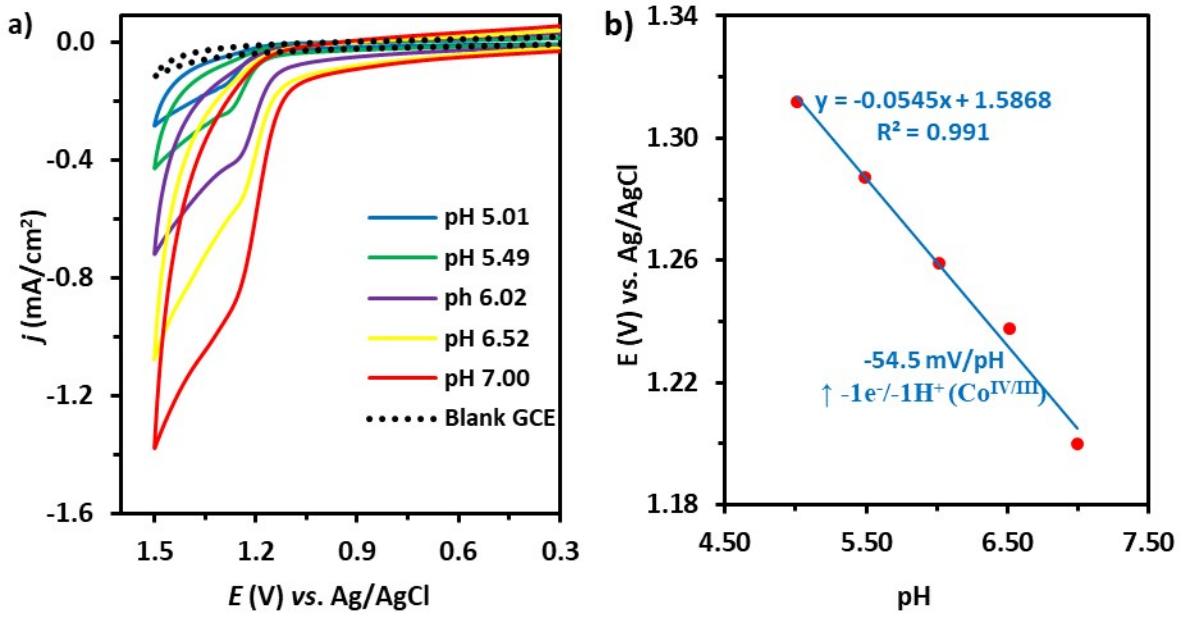

Figure S5. (a) CVs of 1.0 mM vitamin B_{12} in 0.1 M NaPi buffer at different pH values (5.0–7.0) at scan rate of 100 mV/s. The pH of the buffer was adjusted using controlled microvolumetric additions of 1.0 M $NaOH/H_3PO_4$. (b) The plot of the onset potential *vs*. pH value from CV graph.[2, 9, 10]

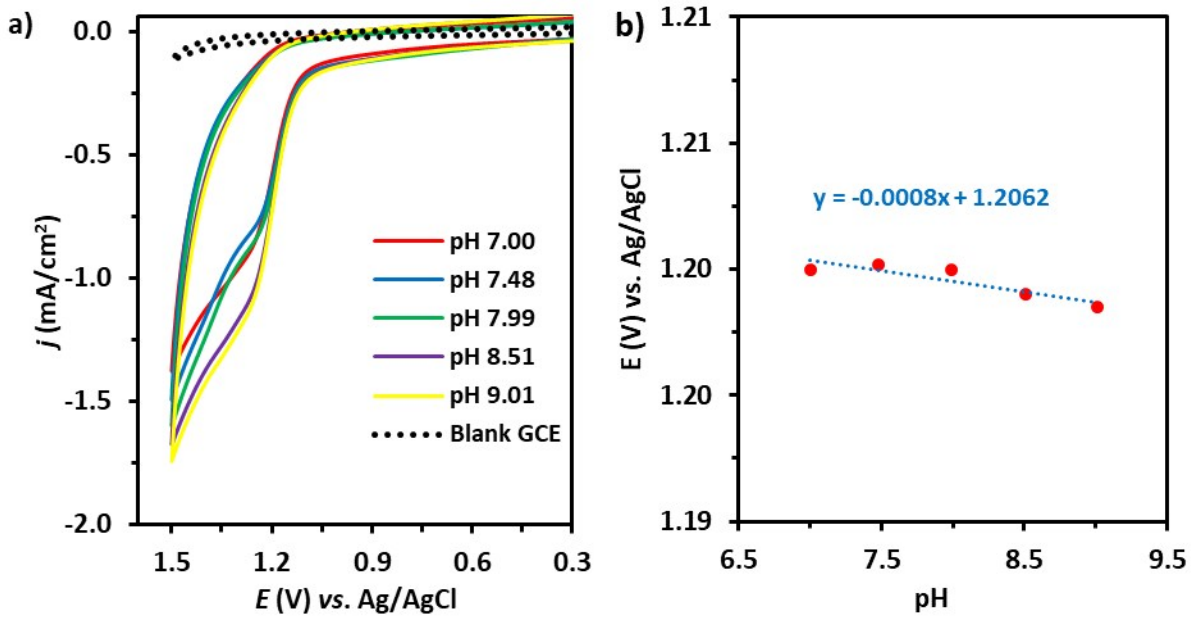

Figure S6. (a) CVs of 1.0 mM vitamin B_{12} in 0.1 M NaPi buffer at different pH values (7.0–9.0) at scan rate of 100 mV/s. The pH of the buffer was adjusted using controlled microvolumetric additions of 1.0 M NaOH/H_3PO_4. (b) The plot of the onset potential *vs*. pH value from CV graph.[2, 9-11]

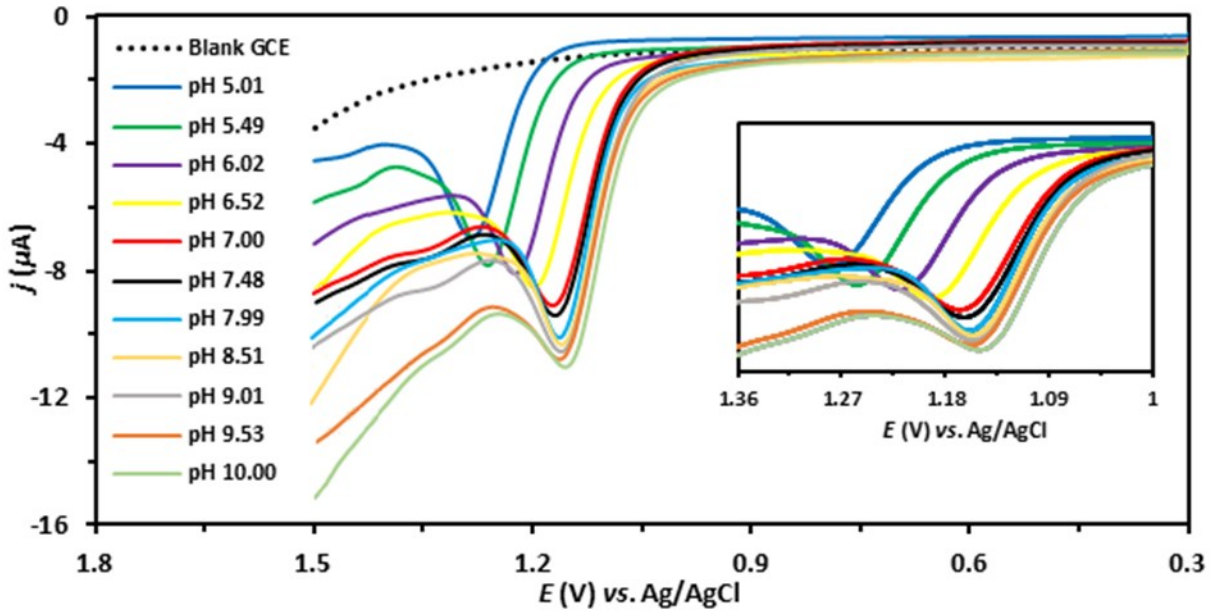

Figure S7. DPV traces in the pH range 5.0 < pH < 10.0 of vitamin B_{12} (1.0 mM) in 0.1 M NaPi buffers for the construction of Pourbaix diagram (Fig. 3 in Manuscript).

In the pH range of 5.0–7.0, the slope of the potential against pH (*ca*. -55 mV/pH) indicates that the redox couple should be a proton-coupled electron transfer (PCET) process, in which proton and electron are transferred in the e^-:H^+ = 1:1 ratio.[9,10] This signals that the CN ligand dissociation followed by water coordination might happen on sweeping the complex at positive

potentials, but before the complex gets oxidized to the higher oxidation state. From the Pourbaix diagram, it could thus be determined that the pK_a value for the cobalt–aqua complex, [Co^{III}-OH_2], is ~7.0. Thus, under acidic and neutral conditions Co^{III}-OH_2 is the dominant species, and the redox process is assumed to be $1e^-$ oxidation coupled with $1H^+$ release to produce the cobalt hydroxo intermediate Co^{IV}-OH. Subsequently, water nucleophilic attack with the release of oxygen will regenerate the starting complex (see Scheme 1). At higher pH values, the dominant species of the complex will be Co^{III}-OH, which undergoes pH-independent oxidation to also generate Co^{IV}-OH.

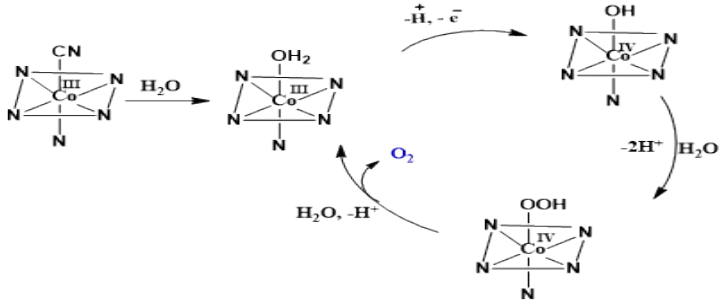

Scheme 1. Proposed mechanism of WO using vitamin B_{12}.

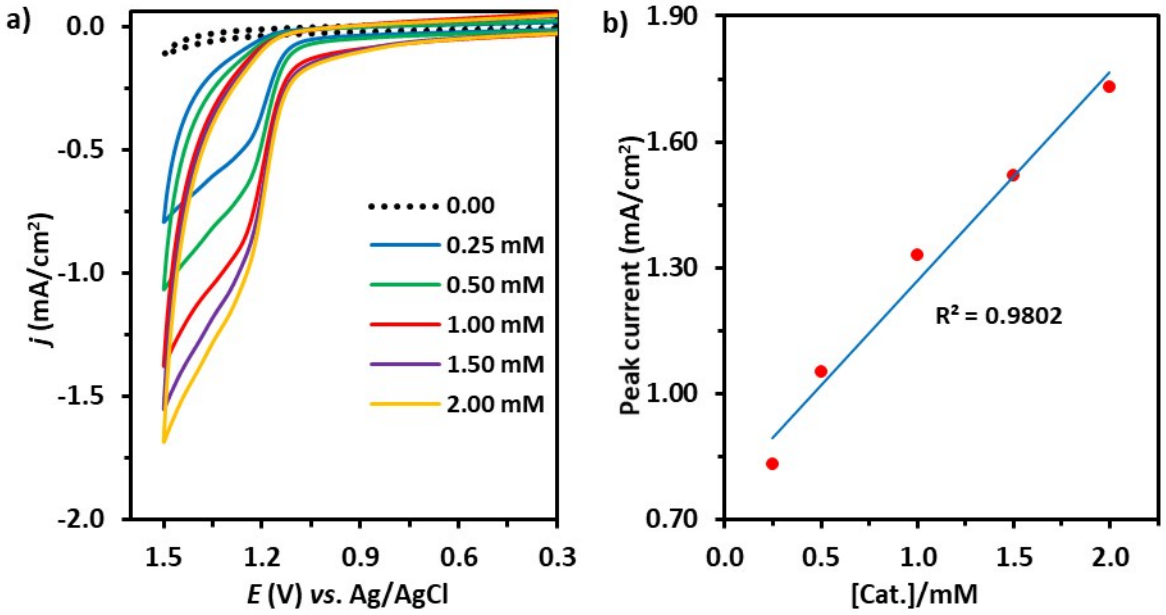

Figure S8. CVs of different concentrations of vitamin B_{12} (0.0~2.0 mM) in 0.1 M NaPi buffer at pH 7.0 with GC electrode (0.07 cm^2) at scan rate of 100 mV/s.[9,11,13]

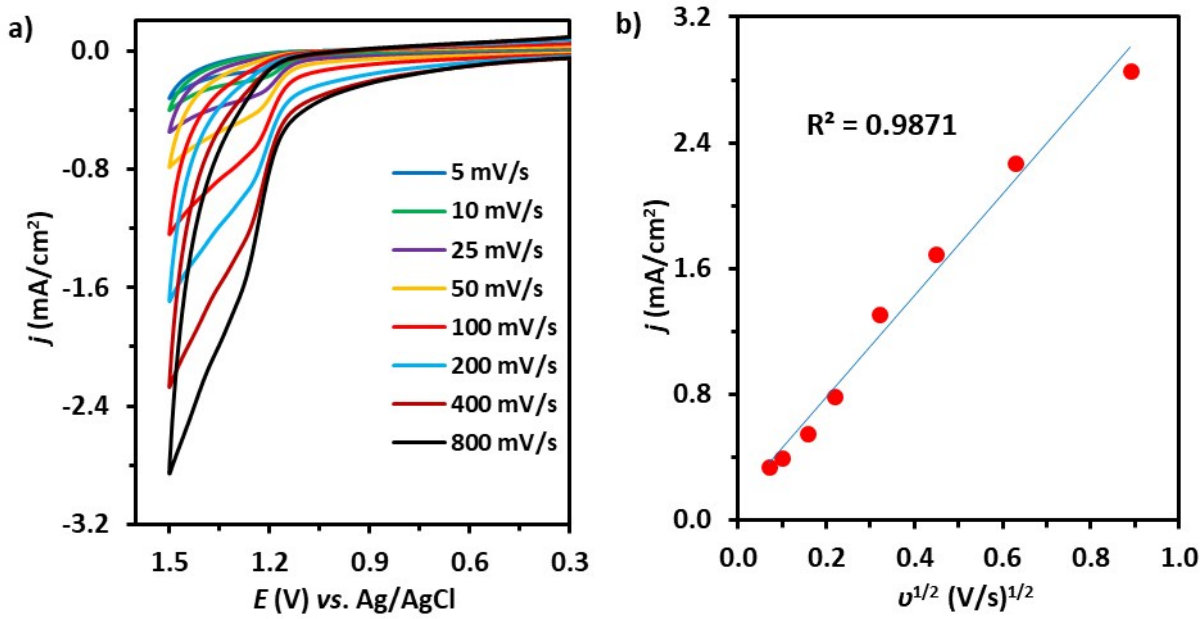

Figure S9. (a) CVs with vitamin B_{12} **(**1.0 mM**)** at different scan rates of 5, 10, 25, 50, 100, 200, 400 and 800 mV/s in 0.1 M NaPi buffer (pH 7.0) with GC electrode (0.07 cm^2).[2,8,14,15] (b) The plot of peak current density *vs*. $\upsilon^{1/2}$ of vitamin B_{12} (1.0 mM) under given conditions.

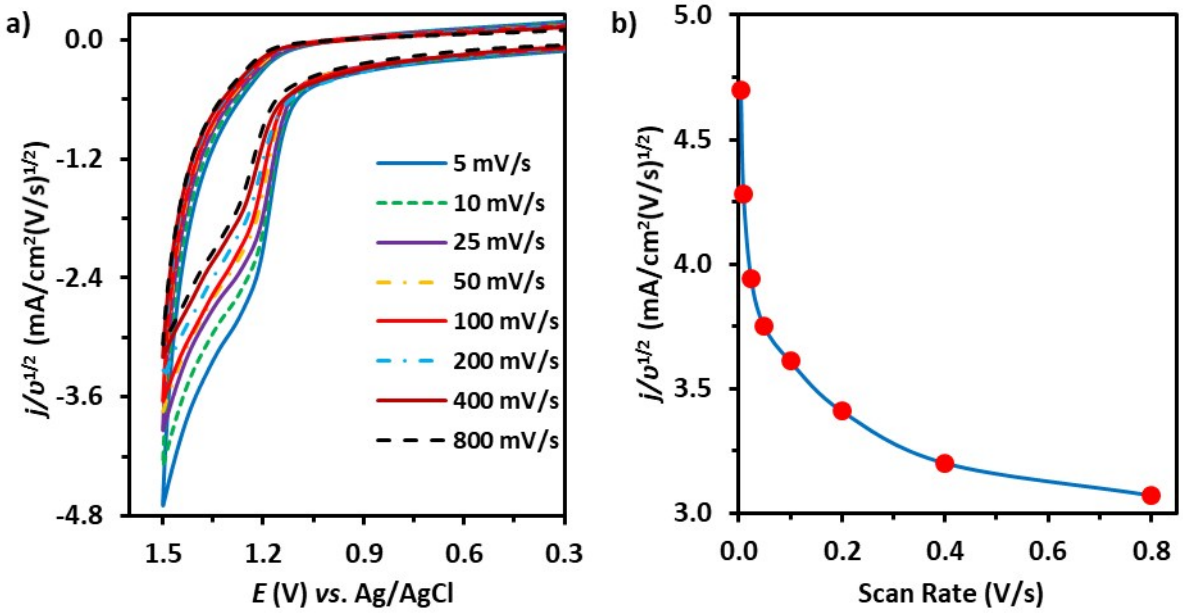

Figure S10. Normalized CVs ($j/\upsilon^{1/2}$) from the CVs of 1.0 mM vitamin B_{12} at different scan rates in 0.1 M NaPi buffer of pH 7.0 (a) and $j/\upsilon^{1/2}$ *vs*. scan rate plot under given conditions (b). The normalized current of the peak at 1.20 V *vs*. Ag/AgCl is independent of the scan rate indicating this is a diffusion-controlled electrochemical behavior. In contrast, the normalized current is reverse dependent on the scan rate, indicating a catalytic behavior happens.[9]

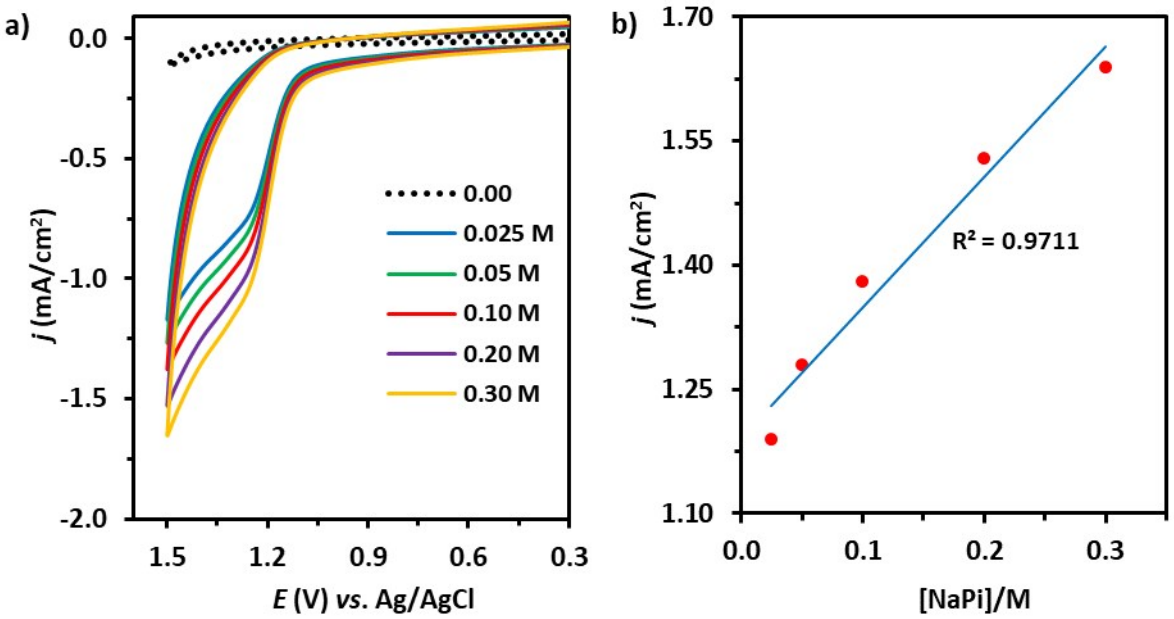

Figure S11. (a) CVs of 1.0 mM vitamin B_{12} with different concentrations of NaPi buffer ([NaPi] = 0~0.3 M; pH was kept constant at 7.0) at 1.50 V *vs*. Ag/AgCl (scan rate = 100 mV/s). (b) Current densities with respect to **[**NaPi] at same condition for representing the linear relationship of current densities and **[**NaPi] at least up to 0.3 M.[16]

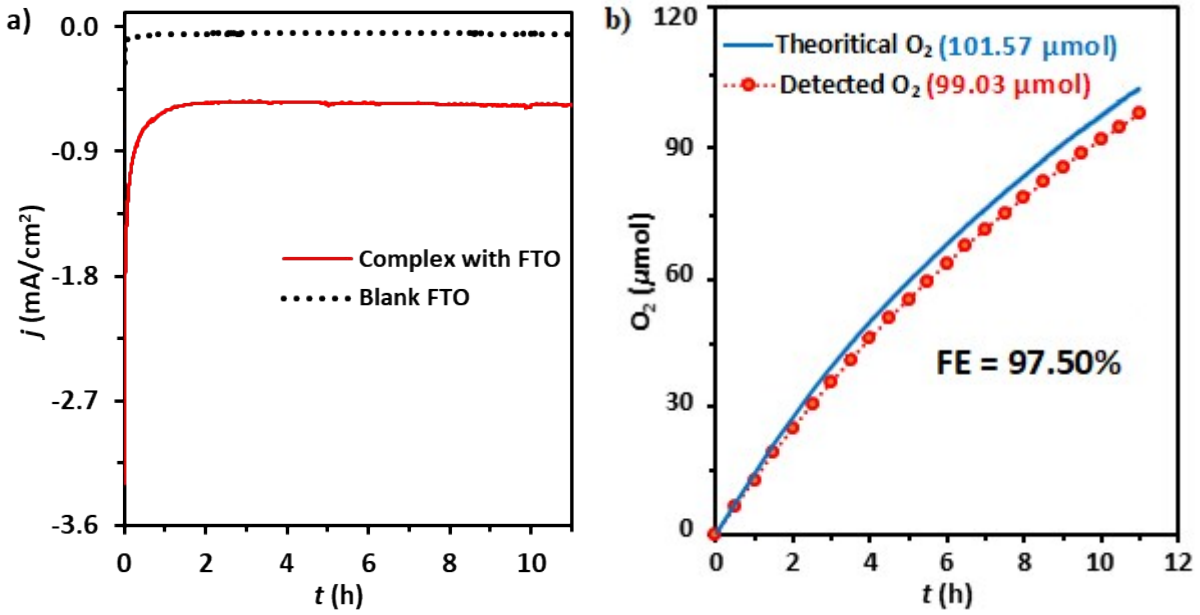

Figure S12. (a) Long–term (11 h) CPE with FTO electrode (*R*s ~7 Ω/sq; 0.8 cm^2) at 1.50 V *vs*. Ag/AgCl containing vitamin B_{12} **(**1.0 mM**)** in 0.1 M aqueous NaPi buffer at pH 7.0. Blank FTO (black; dotted) is shown for comparison. (b) Faradaic efficiency (%) of O_2 evolution for vitamin B_{12} under same conditions in air-tight cell. The dotted red line represents the amount of detected O_2 (DO) quantified by GC-TCD analysis of the gas phase of the system, and the solid blue line indicates the amount of theoretical O_2 (TO) expected for a 100% Faraday efficiency according to the passed charge during CPE experiment.[17,18]

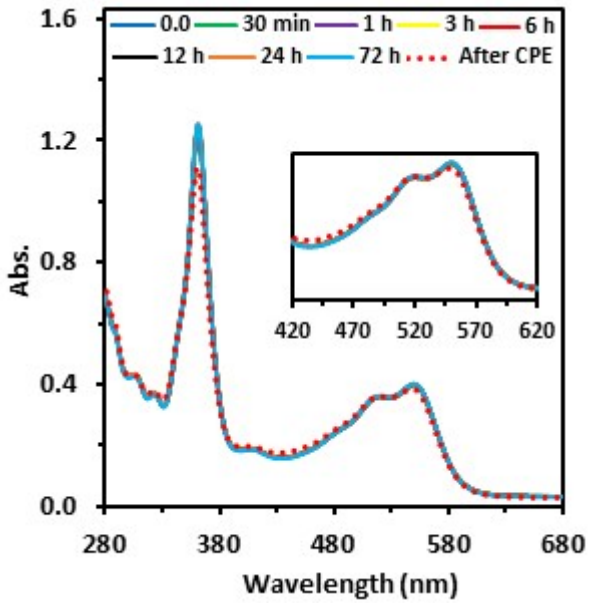

Figure S13. Time–dependent UV–Vis absorption spectra of vitamin B_{12} **(**1.0 mM**)** over 72 h and after long–term CPE (11 h) in 0.1 M NaPi buffer (pH = 7.0) at an applied potential of 1.50 V *vs*. Ag/AgCl.[8]

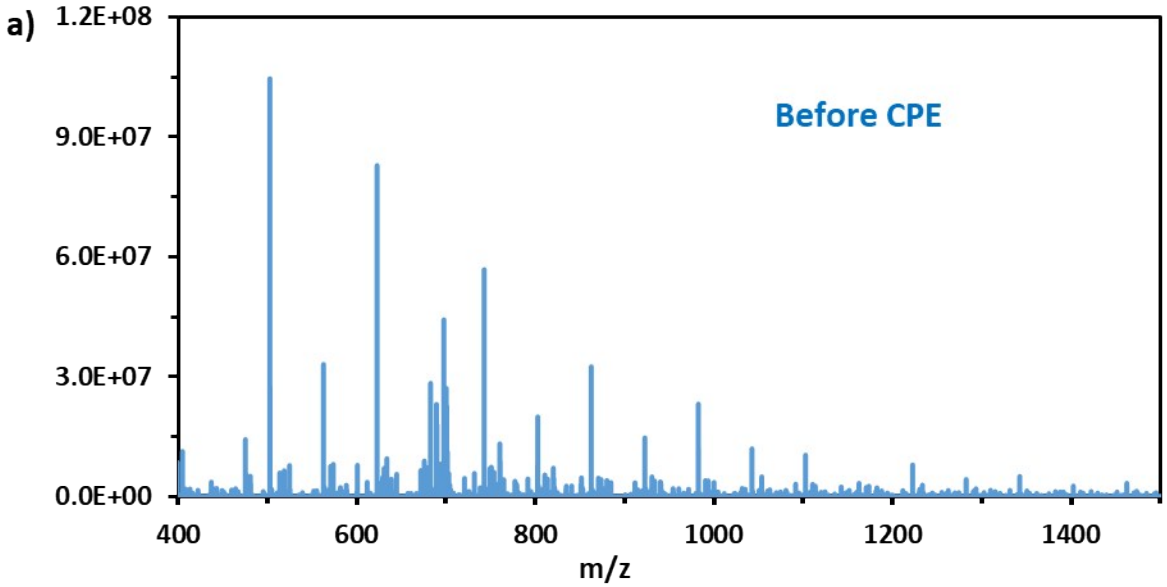

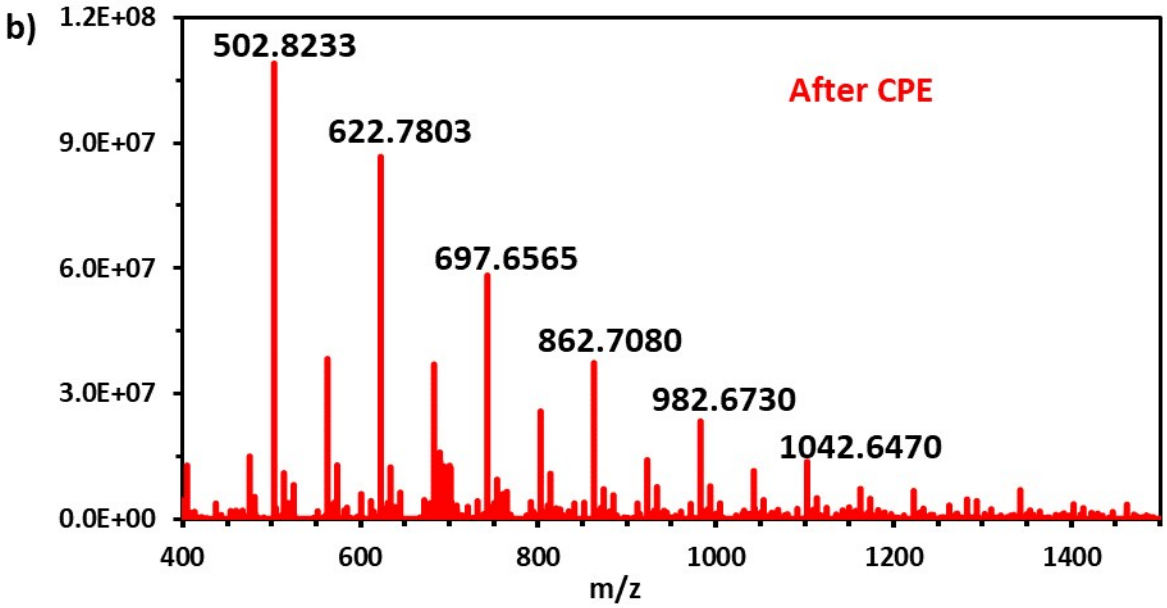

Figure S14. ESI–MS of vitamin B_{12} **(**1.0 mM**)** in 0.1 M NaPi buffer (pH 7.0); before (a) and after (b) long–term CPE at an applied potential of 1.50 V *vs*. Ag/AgCl.[9,19]

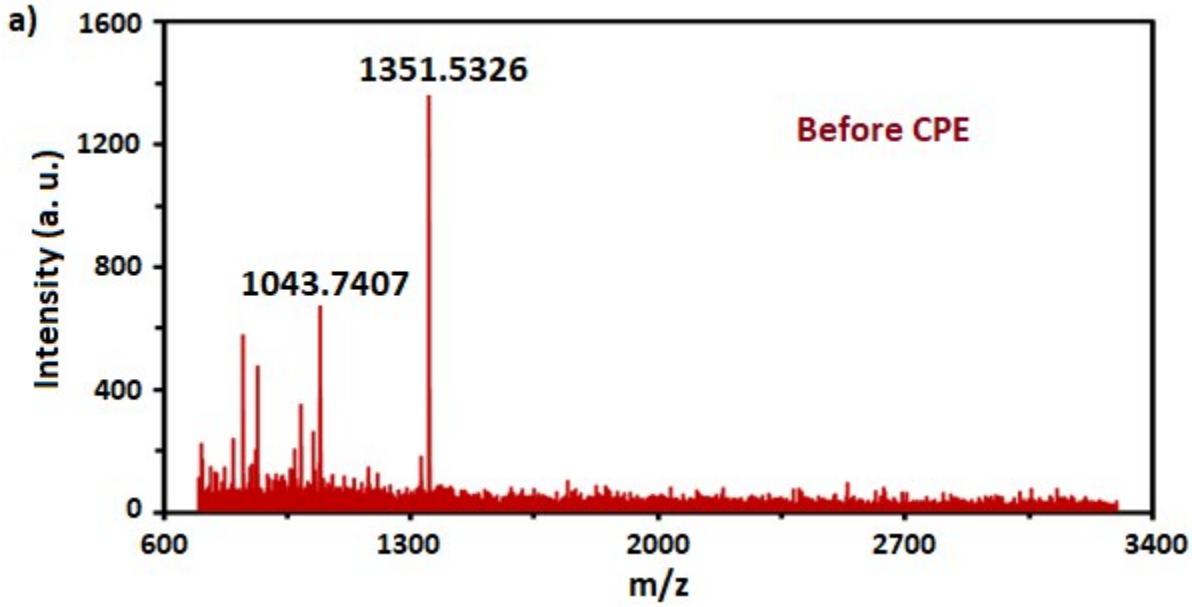

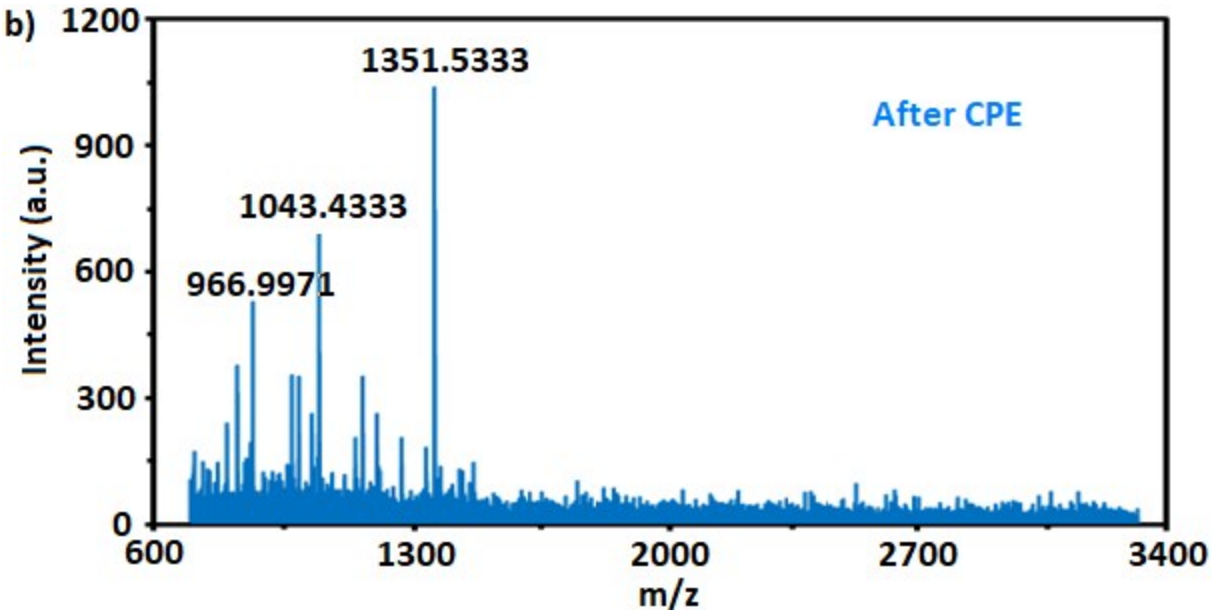

Figure S15. MALDI-TOF–MS of vitamin B_{12} **(**1.0 mM**)** in 0.1 M NaPi buffer (pH 7.0); before (a) and after (b) long–term CPE at an applied potential of 1.5 V *vs*. Ag/AgCl.

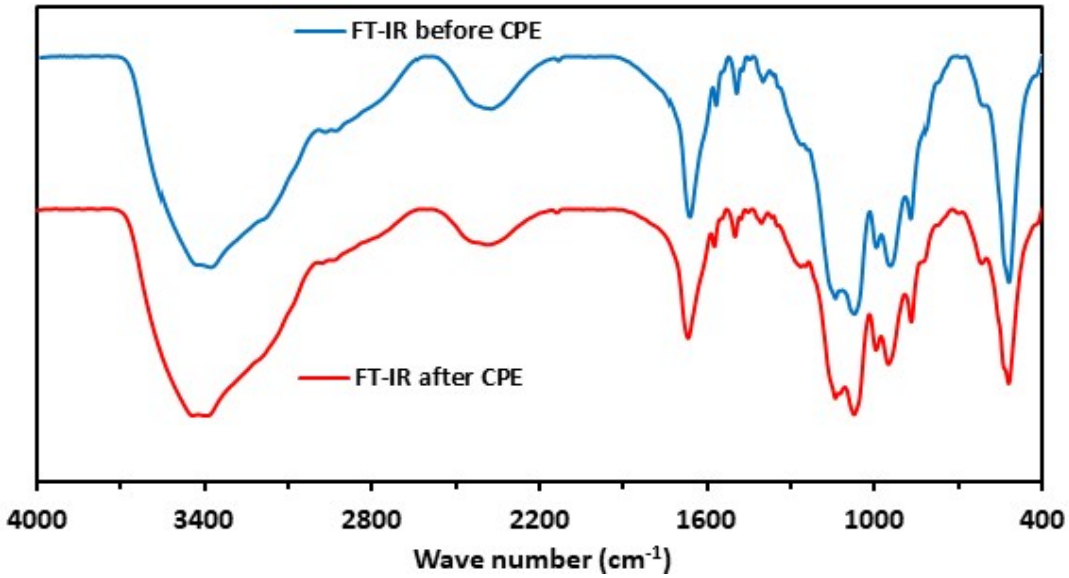

Figure S16. FT–IR spectrum of obtained vitamin B_{12} crystals ranging from 400 to 4000 cm^{-1} at 25 °C for before (blue line) and after (red line) 11 h bulk electrolysis at 1.50 V *vs*. Ag/AgCl.

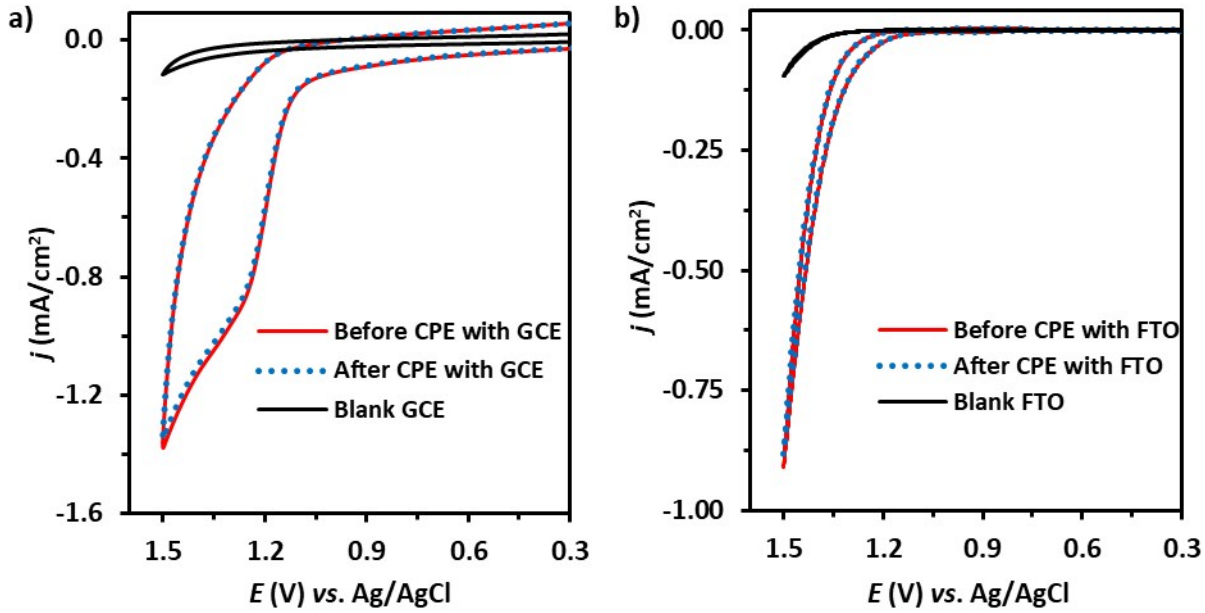

Figure S17. (a) CVs of vitamin B_{12} solution **(**1.0 mM**)** for before (red; solid) and after (blue; dotted) 11 h CPE with GC (0.07 cm^2) electrode (a) and FTO (surface resistivity ~7 Ω/sq; 0.8 cm^2) electrode (b) in blank 0.1 M NaPi buffer (pH 7.0) at scan rate of 100 mV/s. Blank GCE (black; solid) is shown for comparison.[9]

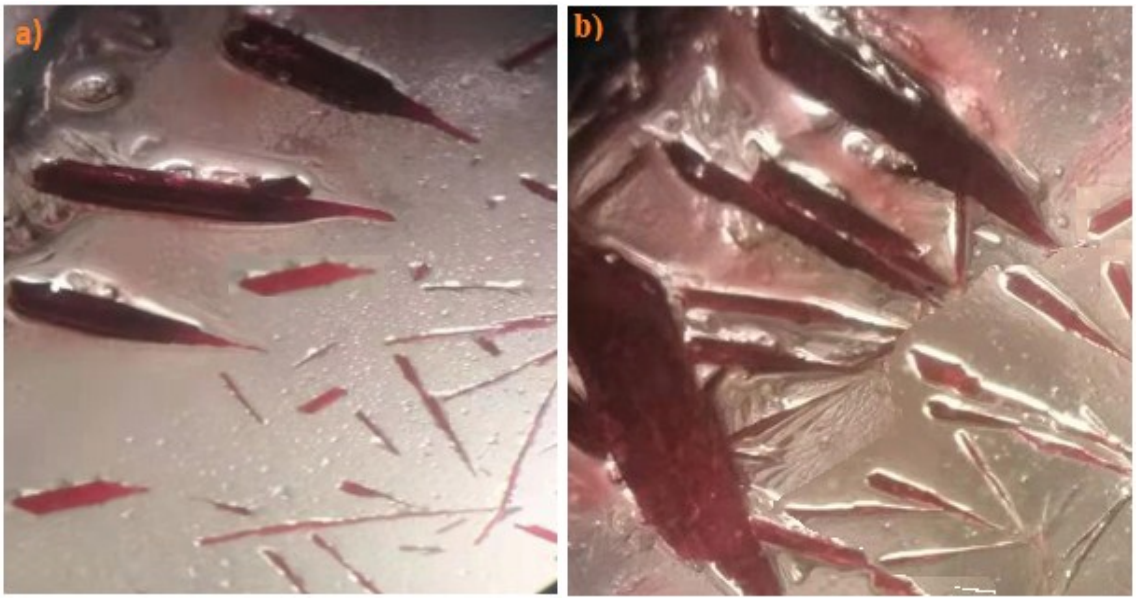

Figure S18. The crystal images of vitamin B_{12} obtained by evaporating the catalyst solution before (a) and after (b) long-term (11 h) CPE at 1.50 V *vs*. Ag/AgCl.[13]

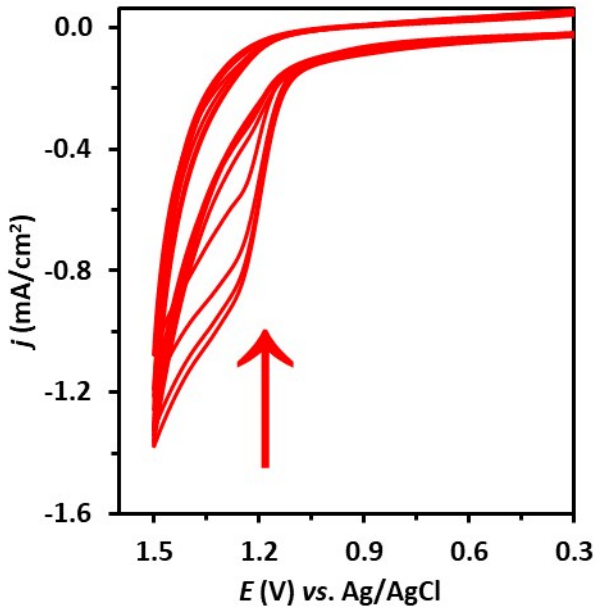

Figure S19. 10 continuous CV cycles of 1.0 mM vitamin B_{12} in 0.1 M NaPi buffers at pH 7.0 with GC electrode (0.07 cm^2) at an applied potential of 1.50 V (scan rate = 100 mV/s).[11, 13]

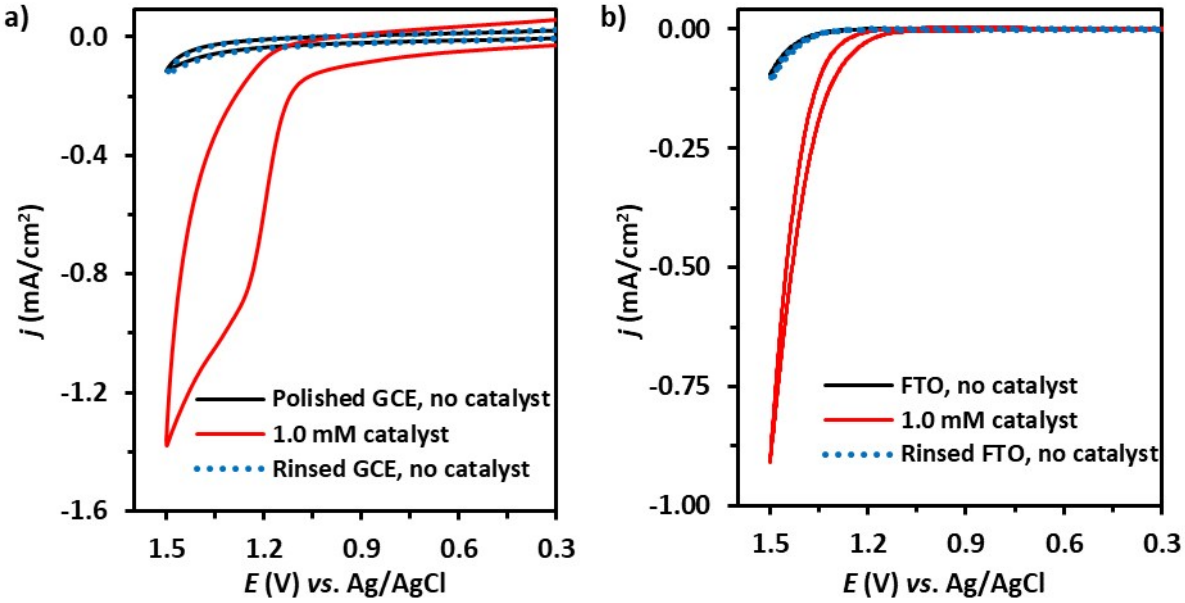

Figure S20. (a) The GC electrode (0.07 cm^2) was cycled 50 times in 0.1 M NaPi buffer (pH 7.0) solution containing vitamin B_{12} **(**1.0 mM**)** catalyst (red; solid) at an applied potential of 1.50 V *vs*. Ag/AgCl (scan rate = 100 mV/s). It was rinsed off, but not polished, then cycled in catalyst–free electrolyte (blue; dotted).[1, 8, 9] (b) The FTO electrode (surface resistivity ~7 Ω/sq; 0.8 cm^2) was cycled in 1.0 mM vitamin B_{12} at pH 9.0 of 0.1 M NaPi buffer (red; solid). After 11 h CPE the FTO electrode was rinsed off and then cycled in a catalyst–free NaPi buffer (blue; dotted). CV was compared to one collected in the same catalyst–free buffer with a polished GC/washed FTO electrode (black; solid).[8, 9, 20]

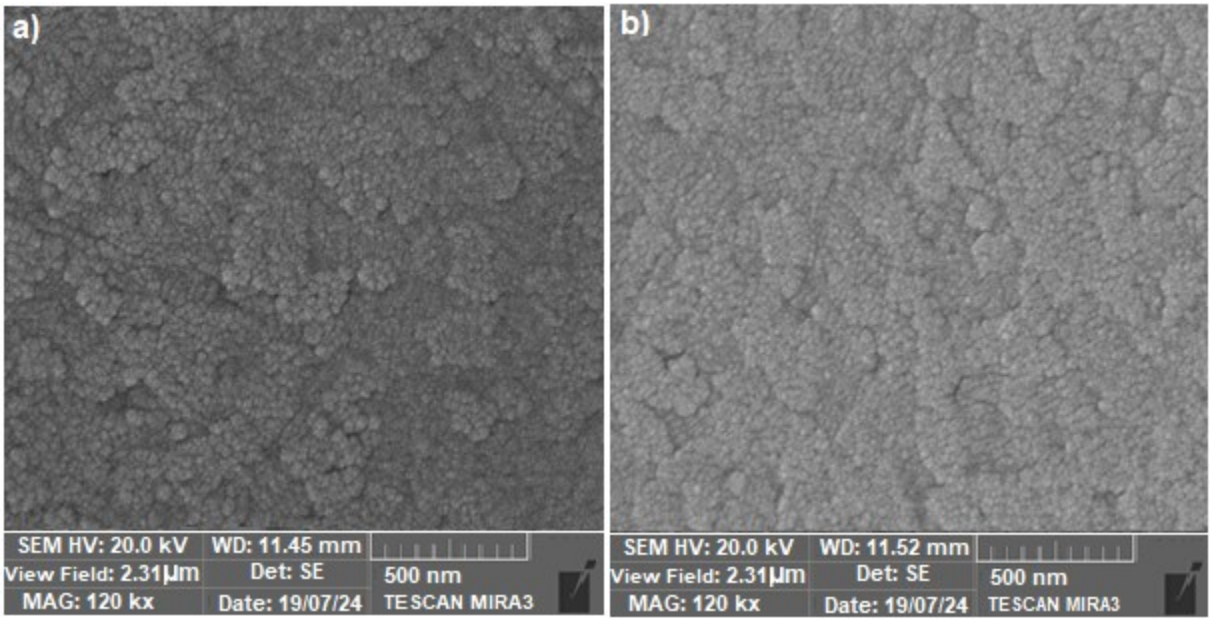

Figure S21. SEM images (500 nm) of FTO (0.8 cm^2) electrodes for before (a) and after (b) 11 h CPE at 1.50 V *vs*. Ag/AgCl (scan rate = 100 mV/s) in 0.1 M NaPi buffer (pH = 7.0) containing 1.0 mM vitamin B_{12}.[2, 9, 20]

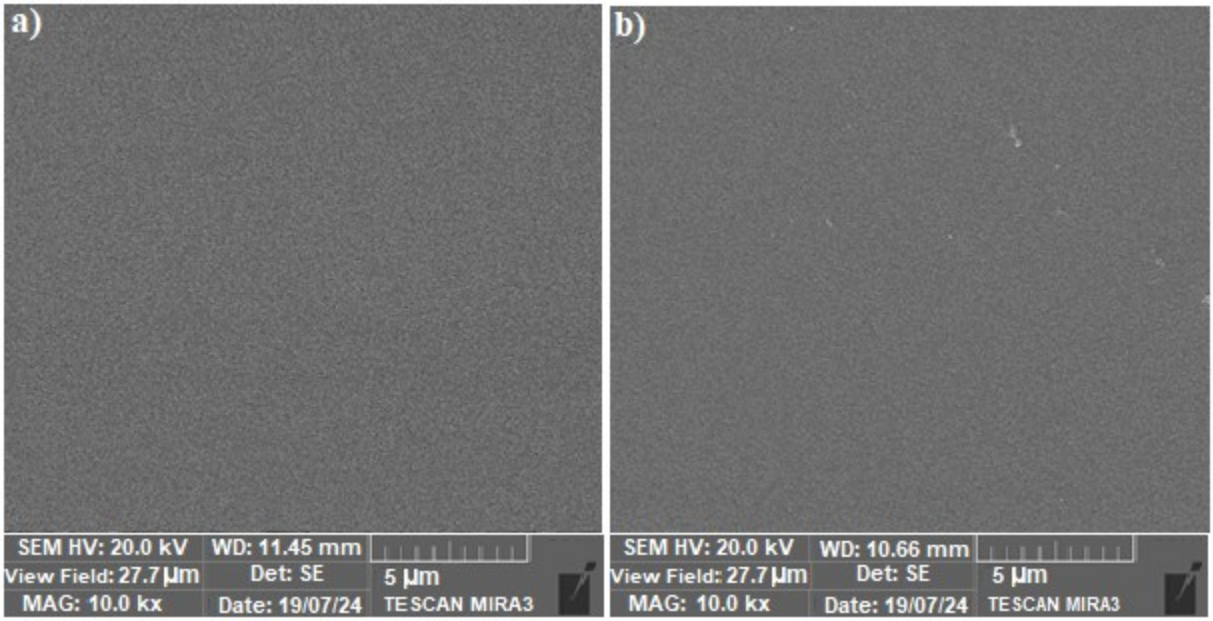

Figure S22. SEM images (5 μm) of FTO (0.8 cm^2) electrodes for before (a) and after (b) 11 h CPE at 1.50 V *vs*. Ag/AgCl (scan rate = 100 mV/s) in 0.1 M NaPi buffer (pH = 7.0) containing 1.0 mM vitamin B_{12}.[2, 9, 20]

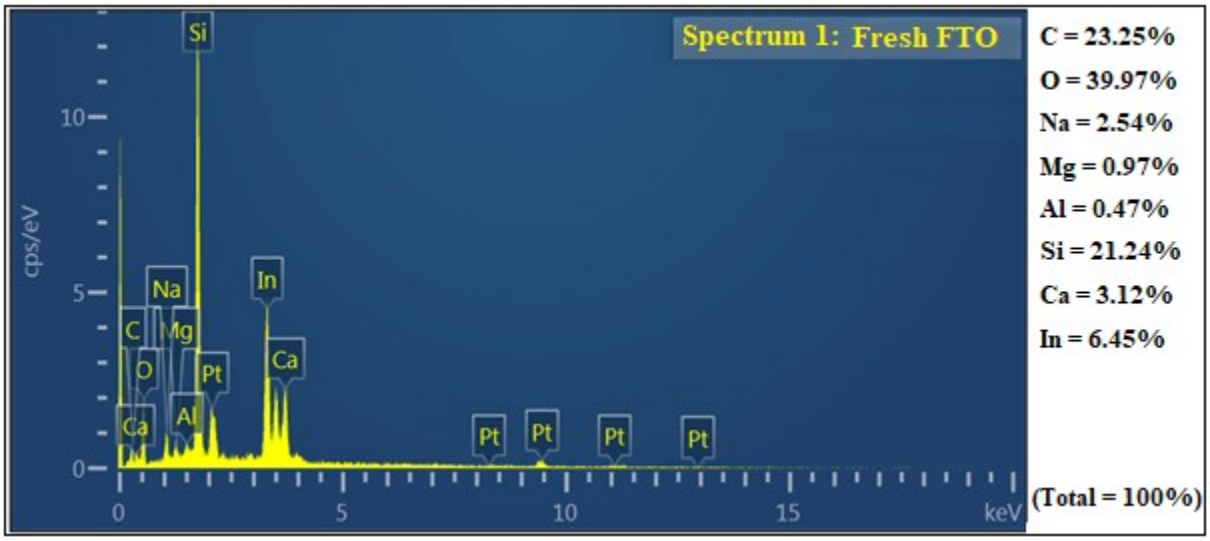

Figure S23. EDX spectrum of the fresh FTO (0.8 cm^2) electrode before electrolysis (Ca, Na, Mg, Al, Si, In, C, and O are from the substrate and Pt is from the coating).

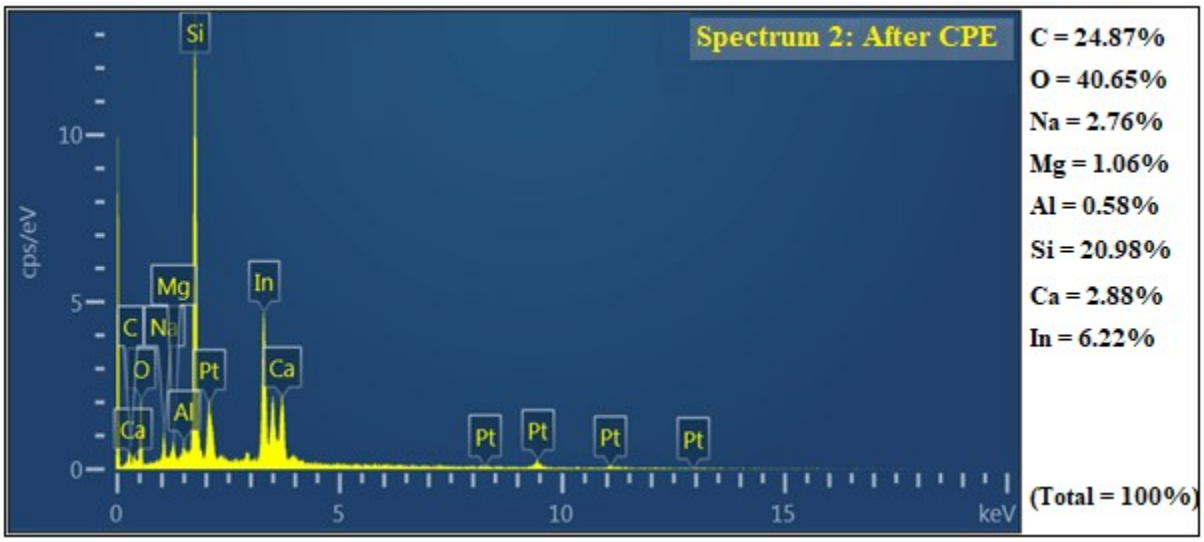

Figure S24. EDX spectrum of the FTO (0.8 cm^2) electrode after 11 h electrolysis at an applied potential of 1.50 V *vs*. Ag/AgCl (scan rate = 100 mV/s) in a 0.1 M NaPi buffer containing vitamin B_{12} (1.0 mM) at pH 7.0. (Ca, Na, Mg, Al, Si, In, C, and O are from the substrate and Pt is from the coating).[2, 9, 20]

References

1. H. Y. Wang, E. Mijangos, S. Ott and A. Thapper, *Angew. Chem. Int. Ed.*, 2014, **53**, 14499-14502.
2. T. Ishizuka, A. Watanabe, H. Kotani, D. Hong, K. Satonaka, T. Wada, Y. Shiota, K. Yoshizawa, K. Ohara and K. Yamaguchi, *Inorg. Chem.*, 2016, **55**, 1154-1164.
3. H. Sun, Y. Han, H. Lei, M. Chen and R. Cao, *Chem. Commun.*, 2017, **53**, 6195-6198.
4. D. Das, S. Pattanayak, K. K. Singh, B. Garai and S. S. Gupta, *Chem. Commun.*, 2016, **52**, 11787-11790.
5. S. Berardi, G. La Ganga, M. Natali, I. Bazzan, F. Puntoriero, A. Sartorel, F. Scandola, S. Campagna and M. Bonchio, *J. Am. Chem. Soc.*, 2012, **134**, 11104-11107.
6. Q. Yin, J. M. Tan, C. Besson, Y. V. Geletii, D. G. Musaev, A. E. Kuznetsov, Z. Luo, K. I. Hardcastle and C. L. Hill, *Science*, 2010, **328**, 342-345.
7. Q. Xu, H. Li, L. Chi, L. Zhang, Z. Wan, Y. Ding and J. Wang, *Appl. Catal. B: Environ.*, 2017, **202**, 397-403.
8. D. Wang and J. T. Groves, *Proc. Natl. Acad. Sci.*, 2013, **110**, 15579-15584.
9. H.-Y. Du, S.-C. Chen, X.-J. Su, L. Jiao and M.-T. Zhang, *J. Am. Chem. Soc.*, 2018, **140**, 1557-1565.
10. T. Ishizuka, A. Watanabe, H. Kotani, D. Hong, K. Satonaka, T. Wada, Y. Shiota, K. Yoshizawa, K. Ohara and K. Yamaguchi, *Inorg. Chem.*, 2016, **55**, 1154-1164.
11. H. A. Younus, N. Ahmad, A. H. Chughtai, M. Vandichel, M. Busch, K. Van Hecke, M. Yusubov, S. Song and F. Verpoort, *ChemSusChem*, 2017, **10**, 862-875.
12. K. S. Joya, N. K. Subbaiyan, F. D'Souza and H. J. de Groot, *Angew. Chem. Int. Ed.*, 2012, **51**, 9601-9605.
13. M. Zhang, M. T. Zhang, C. Hou, Z. F. Ke and T. B. Lu, *Angew. Chem. Int. Ed.*, 2014, **53**, 13042-13048.
14. J. D. Blakemore, N. D. Schley, D. Balcells, J. F. Hull, G. W. Olack, C. D. Incarvito, O. Eisenstein, G. W. Brudvig and R. H. Crabtree, *J. Am. Chem. Soc.*, 2010, **132**, 16017-16029.
15. D. J. Wasylenko, C. Ganesamoorthy, J. Borau-Garcia and C. P. Berlinguette, *Chem. Commun.*, 2011, **47**, 4249-4251.
16. L. Wang, L. Duan, R. B. Ambre, Q. Daniel, H. Chen, J. Sun, B. Das, A. Thapper, J. Uhlig and P. Dinér, *J. Catal.*, 2016, **335**, 72-78.
17. B.-T. Chen, N. Morlanés, E. Adogla, K. Takanabe and V. O. Rodionov, *ACS Catal.*, 2016, **6**, 4647-4652.
18. J. Shen, M. Wang, P. Zhang, J. Jiang and L. Sun, *Chem. Commun.*, 2017, **53**, 4374-4377.
19. B. Huang, Y. Wang, S. Zhan and J. Ye, *Appl. Surf. Sci.*, 2017, **396**, 121-128.
20. H. Liu, M. Schilling, M. Yulikov, S. Luber and G. R. Patzke, *ACS Catal.*, 2015, **5**, 4994-4999.